Maternal Nicotine Exposure Upregulates Collagen Gene Expression in Fetal Monkey Lung

Association with α7 Nicotinic Acetylcholine Receptors

Harmanjatinder S. Sekhon, Jennifer A. Keller, Becky J. Proskocil, Ellen L. Martin, and Eliot R. Spindel

Division of Neuroscience, Oregon Regional Primate Research Center, Beaverton, Oregon; and Department of Pathology, Oregon Health Sciences University, Portland, Oregon

The recent identification of nicotinic acetylcholine receptors (nAChR) in pulmonary fibroblasts suggests that *in utero* nicotine exposure may alter collagen expression by these cells in the developing lung. To test this hypothesis, timed-pregnant rhesus monkeys were administered nicotine (1–1.5 mg/kg/d, subcutaneously) using osmotic minipumps from Days 26–134 or 26–160 of gestation (term = 165 d). *In utero* nicotine exposure significantly increased airway wall area per unit epithelial basement membrane. Collagen type I and III mRNA expression and immunostaining were significantly increased in the airway and alveolar walls of the nicotine-treated group. Elastin mRNA expression increased, but protein expression in parenchyma remained unchanged. Dual labeling studies colocalized α7 nAChR and collagen to the same cells in airway wall cells, and colocalization of α7 nAChR and collagen was confirmed in isolated pulmonary fibroblasts. These findings suggest that nicotine may directly interact with α7 nAChR to increase collagen accumulation in airway and alveolar walls following *in utero* nicotine exposure. These data suggest that passage of nicotine across the placenta to increase collagen deposition and therefore increase airway wall dimensions in fetal lung may partially explain the observed alterations in lung mechanics in the infants of mothers who smoke during pregnancy.

Although a number of studies have shown a strong association between maternal cigarette smoking and spontaneous abortion, preterm delivery, low birth weight, and neonatal morbidity and mortality (1, 2), 10–20% of women still smoke during pregnancy (3). Infants born to mothers who smoke during pregnancy are more prone to respiratory ailments and compromised lung function (4, 5). Epidemiologic studies that have followed children from infancy through childhood have identified significantly increased incidence of bronchitis and hospital admissions for lower respiratory illness in the infants of mothers who smoked during pregnancy, and the correlation is lower with postnatal cigarette smoke exposure than prenatal cigarette smoke exposure (4, 5). Associated with this predisposition to respiratory illnesses are alterations in pulmonary function. A number of studies have reported that infants of mothers who smoke during pregnancy have abnormal lung function tests including decreased lung compliance (6, 7), decreased expiratory flow rates (8–10), increased airway resistance (6, 11), and a decreased ratio of time to peak tidal expiratory flow to total expiratory time (T_{PTEF}:T_E) (7, 8, 12). These changes in lung mechanics that result from *in utero* smoke exposure also persist through late childhood (9) and perhaps even into adulthood (13).

To date, the mechanism by which smoking produces its adverse effects on developing lung remains elusive, but the recent identification of abundant nicotinic cholinergic receptors in developing lung suggests nicotine may be a key factor. This hypothesis is supported by our recent report that prenatal nicotine exposure in monkeys in and of itself alters pulmonary function at birth in very similar ways as smoking during pregnancy alters human infants pulmonary function (14).

The nicotinic cholinergic receptors (nAChR) are ligand-gated ion channels similar to the glycine, γ-aminobutyric acid-a and 5-hydroxytryptamine 3 receptors (15). Nicotinic receptors are pentamers and exist either in heteromeric form composed of both α and β subunits or in homomeric form composed of five of the same α subunit. In brain, the most abundant heteromeric form is $(\alpha4)_3(\beta2)_2$, and the most abundant homomeric form is $(\alpha7)_5$ (15). In developing lung, α7 nAChR are by far the most abundant form of nAChR and are found in airway, vessel, and alveolar wall cells (16). We previously reported a significant upregulation of α7 nAChR expression in fetal monkey lung following maternal nicotine exposure, a finding that suggests a role of α7 nAChR in modulating functional changes in airway and alveolar wall cells in the lung. Consistent with this, we have reported that in rhesus monkeys, maternal nicotine exposure from Days 26–134 of gestation (term = 165 d) alters fetal lung development (16). Lung volume and alveolar surface area are decreased and the size of gas-exchanging units increased in nicotine-exposed fetuses.

Prenatal nicotine exposure strikingly upregulated α7 receptors in what appeared to be fibroblasts surrounding airways and vessels (16). Given that fibroblasts are the primary cells that synthesize lung connective tissues, this suggested that prenatal nicotine exposure may modify collagen expression in developing lung. In lung, collagen types I and III represent 90% of collagen (17). Chambers and Laurent (17) have suggested that whereas collagen I predominantly plays a key role in providing tensile strength, collagen III mainly provides compliance. Nicotine-induced alterations in collagen would thus be consistent with the changes in lung function test in the premature infants observed by Hoo and colleagues (12), who found a decrease in maximal forced expiratory flow and T_{PTEF}:T_E in infants who were exposed to smoke *in utero*. Consistent with this, we have found that prenatal nicotine exposure in monkeys

(*Received in original form August 9, 2001*)

Address correspondence to: Harmanjatinder Sekhon M.D., Ph.D., Division of Neuroscience, Oregon Regional Primate Research Center, 505 NW 185th Ave, Beaverton, OR, 97006. E-mail: Sekhonh@ohsu.edu

Abbreviations: critical threshold, CT; epithelial basement membrane, EpiBM; nicotinic cholinergic receptors, nAChR; phosphate-buffered saline, PBS; ratio of time to peak tidal expiratory flow to total expiratory time, T_{PTEF}:T_E; tris-buffered saline, TBS.

by itself alters pulmonary function at birth as manifested by decreased expiratory flows and increased specific airway resistance (14).

To our knowledge, no study has systematically examined the *in utero* effects of nicotine on connective tissue matrix proteins and possible molecular mechanisms that may be involved in fetal lungs. This study was conducted to address the following issues: *1*) to determine whether nicotine itself may alter the regulation of collagen and elastin gene expression and protein accumulation in fetal lungs, *2*) to determine if α7-nAChR are expressed in pulmonary fibroblasts, and *3*) to determine if maternal nicotine exposure can alter morphometric airway wall dimensions in developing lung.

Materials and Methods

Experimental Design

Experiment 1. Pregnancy in female rhesus monkeys was determined by high blood estrogen and progesterone levels on Days 19, 21, and 23 after mating. Six pregnant female monkeys were randomly divided into control and nicotine treatment groups. On Day 26 of gestation, after confirming pregnancy by ultrasound, Alzet 2ML4 osmotic minipumps (ALZA, Palo Alto, CA) containing nicotine tartrate (Sigma, St. Louis, MO) in normal saline to deliver 1 mg/kg body weight per day were implanted subcutaneously in the midscapular region. Minipumps were changed every 4 wk. Mothers were given food *ad libitum* and weighed routinely to determine untoward effects of nicotine delivery. On Days 92, 106, and 120 of gestation, a sample of amniotic fluid was taken by amniocentesis. Animals received Cefazolin (150 mg twice a day) for 3 d after pump insertion and/or amniocentesis. Control animals did not receive minipumps, but pump insertions were timed to coincide with amniocenteses on Days 92 and 120 to minimize differences in sedative and antibiotic exposure between groups. The studies presented here represent a further analysis of the same animals described in our initial description of the effects of nicotine on fetal monkey lung development (16).

On Day 134 of gestation, fetuses were delivered by cesarean section, and a sample of amniotic fluid was collected to measure nicotine levels. Fetuses were anesthetized and killed by transecting abdominal aorta. Lungs were flushed with normal saline, dissected out, blotted, and weighed. The right lung was ligated, removed, sliced, and fixed overnight either in cold 4% paraformaldehyde in borate buffer (pH 9.5) or in Bouin's fixative. The following day, lung blocks were rinsed in 0.05 M phosphate-buffered saline (PBS) and were either processed and embedded in paraffin or stored at −85°C for future use.

The left lung was fixed with 4% zinc formalin (Sigma) at 20 cm constant transpulmonary water pressure for 3 d. Lung volume was determined by water displacement, and total lung volume was computed using total lung weight. The left lung was sliced in a midsagittal plane into nine blocks, processed, and embedded in paraffin. Sections 5 μm thick from each block were cut and used for morphometric, *in situ* hybridization, and immunohistochemical analyses.

Experiment 2. To allow correlation of structural changes in lung with changes in pulmonary function, a second set of timed-pregnant monkeys was treated with nicotine from Days 26–160 of pregnancy (term = 165 d). On gestation Day 160, fetuses were delivered by cesarean section, kept overnight in the primate center nursery, and subjected to pulmonary function testing the following day and killed for tissue analysis. On Day 26 of gestation, Alzet 2ML4 osmotic mini pumps containing nicotine tartrate dissolved in bacteriostatic water to deliver 1.5 mg/kg/d were implanted subcutaneously in animals in the treatment group, and pumps containing only bacteriostatic water were implanted in animals in the control group ($n = 7$ per group). The pumps were changed every 3 wk until Day 160 of gestation. On Days 118 and 139 of gestation, amniocentesis was performed to obtain a sample of amniotic fluid. All mothers received Cefazolin (150 mg twice a day) for 3 d after pump insertion and/or amniocentesis.

On Day 160 of gestation, fetuses were delivered by cesarean section, and the following day pulmonary function tests were performed, after which the neonatal monkeys were then killed. Lungs were flushed *in situ* with normal saline to remove residual blood from the pulmonary vasculature and were then dissected and processed as described previously. In addition, a portion of right lung was snap frozen for RNA extraction. The nicotine-induced changes in pulmonary function of these animals have been reported by us elsewhere (14).

Fibroblast Isolation

Lungs from a 100-d-gestation rhesus monkey were cut into 1-mm^3 cubes and dissociated for 2 h at 37°C in a solution containing 5 mg/ml Type L collagenase, 5 mg/ml trypsin, and 0.2 mg/ml DNase (Sigma) made in Hanks' balanced salt solution (pH 7.4). The cell suspension was sieved through a sterile 500-μm mesh to remove undissociated tissue and spun at 500 × *g* to pellet dissociated cells. The cell pellet was resuspended and washed twice with RPMI media (supplemented with 10% fetal calf serum, 100 U/ml penicillin, and 100 μg/ml streptomycin). Cells were given 60 min to adhere in a 10-cm^2 culture dish, after which time the media and nonadherent cells were removed and replaced with fresh media.

Immunohistochemical Staining

Tissue sections were deparaffinized and rehydrated through descending series of ethanol and in PBS. After a hot citrate buffer treatment, sections were incubated in 1.5% H_2O_2 and methanol to quench endogenous peroxidase. Nonspecific antigen binding sites were blocked with 3% nonimmune serum, and then primary antibodies rat anti-human α7-nAChR subunit (mAb 319) (18), mouse anti-human collagen type I and type III (ICN Pharmaceuticals, Aurora, OH), and rabbit anti-human α-elastin (Elastin Products, Owensville, MO) were applied overnight at 4°C. On the following day, sections were rinsed with PBS and incubated sequentially with biotinylated secondary antibody and peroxidase-conjugated avidin solution (Vector Laboratories, Burlingame, CA). Peroxidase was visualized with 3-amino-9-ethylcarbazole (AEC) (Vector Laboratories) and counterstained with hematoxylin.

In Situ Hybridization Probe Preparation

Collagen types α1(I), α1(III), α2(V), and elastin cDNA probes for rhesus monkeys were prepared by reverse transcriptase polymerase chain reaction (RT-PCR) using RNA from 140-d fetal monkey lung. Total RNA (5 μg) was reverse transcribed in a 20-μl reaction using an oligo(dT) primer and SuperScript II MMLV reverse transcriptase from Gibco/BRL (Gaithersburg, MD). The reverse-transcribed product was amplified in a standard PCR for 40 cycles of 92° × 1 min, 55° × 30 s, and 72° × 1 min using primers that were highly conserved in human, rabbit, and rat to produce collagen type I, collagen type III, and elastin cDNAs. For collagen mRNA α1(I), a 562-bp cDNA was amplified using the 5′ and 3′ primers CCC CCT GGA AAG AAT GGA GAT GAT G and GGA AGC CAG GAG CAC CAG CAA TAC CAG; for collagen mRNA α1(III), a 426-bp cDNA was amplified using the 5′ and 3′ primers CCC TGG AAT CTG TGA ATC ATG CCC TAC and CCT GTT TCA CCC TTT TCT CCA TTT CGT; for collagen mRNA α2(V), a 412-bp cDNA was amplifed using the 5′ and 3′ primers AGC CCG CAC GTG TGA TGA CCT AA and CAT TTG CCC CTT TGA GAA CCA CA. The elastin cDNA was amplified using 5′ and 3′ primers TGG AGG CAA

ACC TCT TAA GCC AGT TCC and GCA GTC CAT AGC CAC CAG GCA GCT TGG. cDNA bands of the appropriate size were subcloned into pGEM-T, mini-prepped (Perfect preps, 5′prime-3′prime, Boulder, CO) and sequenced. Sequence was obtained on at least two independent subclones to eliminate any PCR errors. The partial cDNA sequences have been deposited in Genbank, and the accession numbers are AF230925, AF230926, and AF230927, respectively.

In Situ Hybridization

In situ hybridization was done as described previously (16). In brief, zinc-formalin–fixed tissue sections were deparaffinized in xylene and rehydrated in ethanol. Sections were incubated with 20 μg/ml proteinase K (0.1 M tris, 0.05 M EDTA, pH 8.0) for 20 min and 0.1 M triethanolamine and acetylated with 0.0025% acetic anhydride. After slides were rinsed in 2× SSC, they were dehydrated in ascending series of alcohol and vacuum dried. Thereafter, ^{35}S-radiolabeled cRNA probes were applied to slides, which were sealed in humidified chambers and incubated at 55°C for 16 h. Slides were treated with RNase-containing buffer (20 μg/ml RNASE A, 0.5 M NaCl, 0.01 M tris, 1 mM EDTA; pH 8.0) at 37°C for 30 min to inactivate nonhybridized probe, rinsed in descending series of SSC (2× SCC, 1× SSC, 0.5× SSC) containing 0.1 M DTT, and incubated in 0.1× SSC and 0.1 M DTT at 65°C for 30 min. Sections were dehydrated in alcohol, vacuum dried, coated with NBT2 autoradiographic emulsion (Kodak, Rochester, NY), stored at 4°C for 2 wk, developed, and counterstained with hematoxylin.

Dual Immunohistochemistry and *In Situ* Hybridization

Dual labeling was performed to determine if α7 nAChRs were expressed in the same cells expressing collagen III mRNA. Immunohistochemical staining was done as described previously except that sections were stained with 3,3′diaminobenzidine. After immunohistochemical staining, sections were treated with proteinase K (20 μg/ml) for 15 min, and the protocol described previously was used for hybridization with the ^{35}S-collagen type III cRNA probe.

Dual α-Bungarotoxin Binding and Collagen Immunohistochemistry

Bouin's fixed tissue sections were deparaffinized, rehydrated in tris-buffered saline (TBS) for 20 min, and incubated with nonspecific binding buffer (TBS + 0.2% bovine serum albumin + 2% nonimmune horse serum) for 1 h at room temperature. Sections were incubated overnight with the collagen III monoclonal antibody described previously at 4°C. After rinsing with TBS, sections were either treated with binding buffer alone or containing 5 mM nicotine at room temperature for 1 h. Thereafter, a mixture of 15 nM Texas Red conjugated α-bungarotoxin (Molecular Probes, Eugene, OR) and fluorescein–conjugated, anti-mouse antibody (Vector Labs, Burlingame, CA) was applied to the sections and incubated for 3 h at 37°C. The sections were rinsed three times in TBS, and nuclei were counterstained using Vectashield mounting media containing 4′,6-diamidino-2-phenylindole (DAPI) (Vector Labs, Burlingame, CA). Colocalization was determined using a confocal microscope (Leica, Mannheim, Germany).

Morphometry and Image Analysis

Alterations in airway wall dimensions, collagen and elastin mRNA expression, and collagen and elastin protein expression following nicotine treatment were determined using MetaMorph Imaging System software (Universal Imaging, West Chester, PA). Images were acquired with a DKC-5000 camera (Sony, Tokyo, Japan). Collagen type I and III mRNA expression was measured in cartilaginous and noncartilaginous airways. Collagen protein expression was measured in cartilaginous, membranous, and terminal airways. Elastin mRNA expression was measured only in parenchyma because its expression was low in airway walls. Airway wall thickness was determined in H&E-stained sections. An average of multiple measurements at the narrowest airway lumen was calculated as representative of airway size. Airway wall was digitized excluding airway epithelium, cartilage, and submucous glands, and wall area was determined. A corresponding segment of subepithelial basement membrane was also digitized and was used as a reference length to normalize airway wall area.

In Situ Hybridization Image Analysis

Using multiple dark-field images from at least one section from each animal (a total of 20–25 images), the luminosity threshold was set to identify silver grains for each probe individually and applied to all images of each individual probe included for analysis. Using the same images, an average of grain intensity and area was determined by for each mRNA probe individually and used for computations. Simultaneously acquired bright- and dark-field images were used to measure mRNA expression. The bright-field image was used to digitize the area of the region of interest, and that area was then transposed onto the concordant dark-field image for grain counting. In case of cartilaginous airways, cartilage and submucous glands were not included in analysis. Signal background for the individual slide was subtracted, and a total number of grains in a region of interest was computed. In airways, the length of the corresponding subepithelial basement membrane was also measured and used to calculate the number of silver grains per unit epithelial basement membrane. A total number of grains per unit airway wall area was computed.

To assess mRNA expression in parenchyma, 20 randomly selected fields consisting only of primitive alveolar structures or alveolar ducts were included for analysis in each animal. As explained previously, the total number of grains of each field was determined, and an average of the total number of grains per unit area was calculated. Because the sizes of primitive alveolar units were not similar, the total number of grains per unit area was also corrected for volume density of alveolar wall determined by standard morphometric techniques described elsewhere (16).

Immunohistochemical image analysis. Semi-quantitation of collagen and elastin protein expression was made using immunostained sections. Following peroxidase reaction, AEC imparts red color; only the red channel was used to determine the color intensity of staining. For each immunohistochemical stain (collagen type I and III and elastin), three or four randomly selected sections from the control and treatment groups were processed in parallel using nonimmune serum instead of primary antibody. Using these sections, multiple random images of representative lung structures were obtained for each individual stain and used to determine the average baseline color threshold. The average baseline color threshold was applied to all images for each individual immunostain. The regions of interest were digitized, and color intensity was measured. Airway wall area and the corresponding length of epithelial basement membrane were measured as described previously. The integrated intensity (expressed in arbitrary units) of the selected area was expressed as per unit basement membrane and per unit area for individual airways. In case of partially or tangentially cut airways, walls along the shortest diameter were included for analysis. Only those terminal airways where a distal continuation to respiratory bronchiole and alveolar ducts was found were included for measurement. As described earlier, for assessment of collagen and elastin protein expression in parenchyma, 20 random fields containing only gas exchanging units were used to measure color intensity in each animal. After subtracting background, the average measurement of all fields for each animal was determined and corrected for morphometrically determined volume density of the alveolar wall.

Real-time PCR mRNA Analysis

Real-time PCR was used to quantify collagen I, III, and V mRNA levels. RNA samples were prepared for real-time PCR by random-

primed reverse transcription reaction using reagents from Applied Biosystems (Foster City, CA) and 1 μg of RNA. The reverse transcription reaction was then diluted 1:500 for PCR analysis. Primers and probes were designed using the Primer Express software (Applied Biosystems). The 10-μl PCR reaction consisted of 5 μl TaqMan Universal PCR Master Mix, 2 μl probe/primer mix, and 3 μl diluted RT reaction. Reactions were conducted in triplicate for increased accuracy. After PCR was completed, baseline and threshold values were set to optimize the amplification plot, and the data were exported to an Excel spreadsheet. A standard curve was drawn on the basis of the log of the input RNA versus the critical threshold (CT) cycle, which is the cycle in which the fluorescence of the sample was greater than the threshold of baseline fluorescence. This standard curve allowed for the CT values to be converted to relative RNA concentrations for each sample. Figure 6A shows the standard curve used for the collagen I mRNA analysis. RNA levels were normalized to the level of 18S RNA expression for each sample using 18S primers and probe on the same template cDNA.

Statistical Analysis

Means and standard errors of means were calculated using Number Cruncher Statistical System (Kaysville, UT). Pairwise differences between means of treatment and control groups were analyzed by *t* test. For analysis of nicotine's effects on collagens I, III, and V, levels were expressed as percentage of control and analyzed by one-way ANOVA.

Results

On Day 26 of gestation, Alzet mini-osmotic pumps containing saline or nicotine were implanted subcutaneously. Neither food intake nor maternal weight gain was affected adversely by nicotine treatment. As described previously, at the time of cesarean section on Day 134 of gestation, amniotic fluid nicotine levels were 15.4 ± 3.8 ng/ml (16). Body weight of 134-d fetuses in the nicotine-exposed group was lower than in the control group (323.3 ± 8.9 versus 348.9 ± 26.1 g) but did not reach statistical significance.

Airway Thickness

Nicotine induced changes in airway wall thickness at all levels of airways following nicotine exposure in 134-d fetuses. Net airway wall area (total airway wall area excluding cartilage and submucous glands area) per unit epithelial membrane increased significantly in fetuses exposed to nicotine during gestation. Categorically, cartilaginous airway wall thickness increased by 17%, membranous airways by 17%, and terminal airways by 22% compared with the control group (Table 1). Linear regression analysis of airway wall thickness per unit epithelial basement membrane and airway diameter also showed significant differences (nicotine $R^2 = 0.47$, slope 0.126, and Y intercept 29.9 versus 0.55, 0.098, and 16.5, respectively, in the control group) between nicotine-treated and control groups ($P < 0.0001$).

Airway Collagen, Elastin, and α7 nAChR Expression

In the cartilaginous airways, collagen type I and type III mRNA expression was predominantly localized in the extracartilaginous layer and particularly in the high fibroblast density paracartilaginous regions. In cartilaginous airways, collagen α1(I) and α1(III)mRNA expression was upregulated following nicotine exposure (Figures 1A–1D). As shown in Figures 1E and 1F, collagen immunohistochemical staining showed a similar expression pattern as the mRNA and was similarly upregulated by nicotine. Immunohistochemical staining distribution was similar to that of mRNA expression in the extracartilaginous areas including the smooth muscle cell layer in the large airways and was widely distributed in the membranous airway walls. The distribution of α7 nAChR expression was similar to that of collagen expression, and α7 nAChR expression increased in a pattern similar to collagen mRNA after nicotine exposure (Figures 1G and 1H). By immunohistochemistry no other nicotinic receptor subtypes (α3, α5, α6, β2, β3, or β4) were detected in the paracartilaginous region (data not shown).

The effect of nicotine on collagen mRNA in different-sized airways was quantified by image analysis of the *in situ* hybridization analyses (Figures 2 and 3). In cartilaginous airways, collagen α1(I) mRNA expression was significantly upregulated following nicotine exposure (Figures 2A and 2B). The number of grains per unit epithelial basement membrane (EpiBM) and per unit area significantly increased (88 and 62%, respectively) compared with controls. In noncartilaginous airways, nicotine similarly increased collagen type I mRNA levels (Figures 2A and 2B). Collagen α1(III) mRNA levels per unit EpiBM and per unit area also increased significantly both in cartilaginous (88 and 48%, respectively) and in noncartilaginous (96 and 76%, respectively) airways (Figures 3A and 3B). No measurements were made for airway elastin mRNA levels because the expression was low and remained unaffected by nicotine exposure.

Image analysis was also performed to quantify immunohistochemical staining for collagen in different-sized airways. Collagen type I immunostaining intensity per unit

TABLE 1

Effect of prenatal nicotine exposure on fetal cartilaginous and noncartilaginous airway wall dimensions

Parameter	Control	Nicotine	*P* Value
Cartilaginous airway wall area/ μm epithelial basement membrane	64.52 ± 3.74* ($n = 16$)	75.84 ± 4.47 ($n = 22$)	0.036
Membranous airway wall area/ μm epithelial basement membrane	26.28 ± 0.93 ($n = 15$)	30.76 ± 1.49 ($n = 21$)	0.013
Terminal airway wall area/ μm epithelial basement membrane	18.62 ± 0.94 ($n = 18$)	22.89 ± 1.21 ($n = 22$)	0.005

* Values are means ± SE.

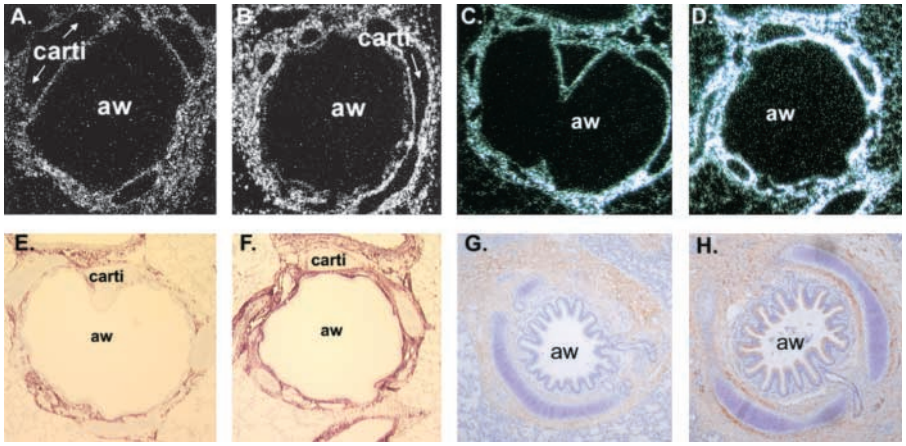

Figure 1. Effect of prenatal nicotine exposure on collagen and α7 nAChR in cartilaginous airways. (*A*) Antisense ^{35}S-labeled cRNA probe showing collagen α1(I) mRNA expression in lung from a control 134–d fetal monkey. (*B*) α1(I) mRNA expression in lung from a nicotine-exposed, 134–d fetal monkey. Little hybridization was seen in sense controls (data not shown). (*C* and *D*) Collagen α1(III) mRNA expression in control and nicotine-exposed, 134–d fetal lung. (*E*) Collagen III immunostaining of control 134-d fetal lung using a collagen type III monoclonal antibody. Chromogen = AEC (*red color*; *see* MATERIALS AND METHODS). (*F*) Collagen III immunostaining of nicotine-exposed fetal lung. (*G*) α7 nAChR immunostaining of 134-d fetal lung using monoclonal antibody 319 (chromogen = AEC, *red color*). (*H*) α7 nAChR immunostaining of 134-d nicotine-exposed lung. Lung tissue for panels *A–F* was from tissue fixed in zinc formalin and inflated to 20 cm pressure. Because of antibody requirements, panels *G* and *H* were fixed in Bouins and were not inflated, hence difference in appearance of the airway lumens. All sections shown at 100× magnification.. aw, airway; carti, cartilage.

EpiBM and per unit area in cartilaginous airways increased by 48% ($P = 0.01$), in membranous airways by 50% ($P = 0.007$), and in terminal airways by 366% ($P < 0.001$) (Figure 2C). In addition, collagen type I protein expression was also increased per unit area in cartilaginous (42%; $P = 0.0004$), membranous (35%; $P = 0.01$), and terminal (266%; $P < 0.001$) airways in the nicotine-treated group compared with the control group (Figure 2D).

The intensity of collagen type III staining normalized for epithelial basement membrane and airway wall area also increased significantly in cartilaginous airways (51 and 42%, respectively), membranous airways (125 and 128%, respectively), and terminal airways (427 and 349%, respectively) following nicotine exposure compared with controls (Figures 3C and 3D).

Parenchymal Collagen and Elastin Expression

Collagen mRNA expression and immunostaining was widely distributed throughout the parenchyma (Figure 4). By contrast, elastin staining was mostly concentrated at and

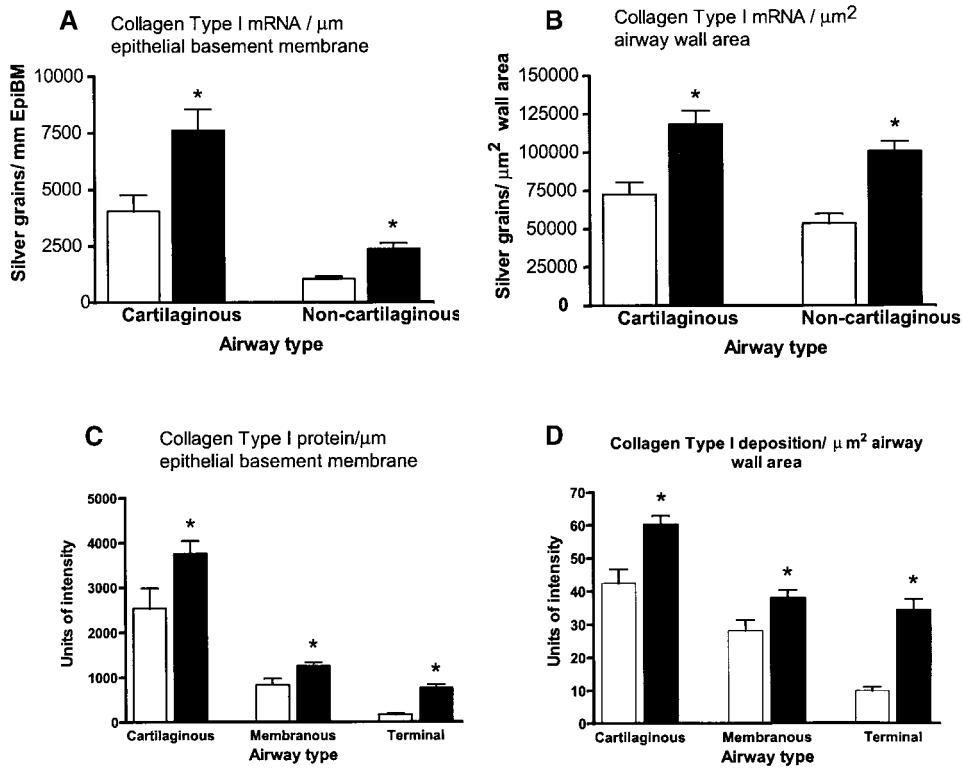

Figure 2. Effect of maternal nicotine on collagen type I in fetal lung. (*A*) mRNA expression in cartilaginous (control, $n = 24$; nicotine, $n = 29$) and noncartilaginous (control, $n = 35$; nicotine, $n = 41$) airway wall per unit epithelial basement membrane. (*B*) mRNA expression in cartilaginous (control, $n = 24$; nicotine, $n = 29$) and noncartilaginous (control, $n = 35$; nicotine, $n = 41$) airway wall per unit wall area. (*C*) Protein expression in cartilaginous (control, $n = 13$; nicotine, $n = 21$) and membranous (control, $n = 10$; nicotine, $n = 12$) and terminal (control, $n = 17$; nicotine, $n = 15$) airway wall per unit epithelial basement membrane. (*D*) Protein expression in cartilaginous (control, $n = 13$; nicotine, $n = 21$) and membranous (control, $n = 10$; nicotine $n = 12$) and terminal (control, $n = 17$; nicotine, $n = 15$) airway wall per unit wall area. $^*P < 0.05$. *Open bars*, control; *solid bars*, nicotine.

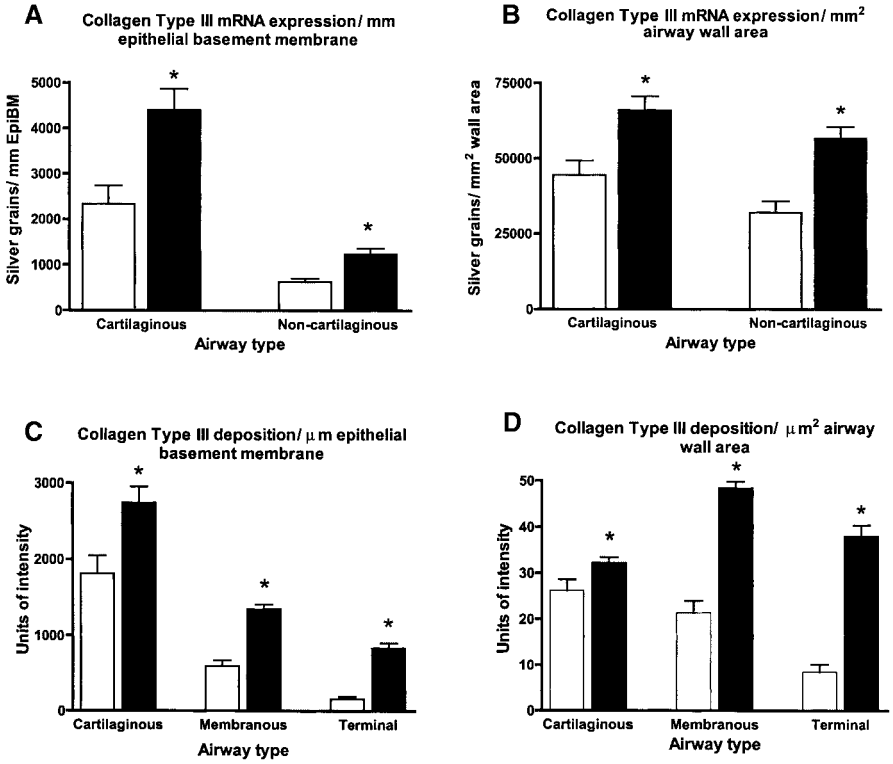

Figure 3. Effect of maternal nicotine on collagen type III in fetal lung. (*A*) mRNA expression in cartilaginous (control, n = 22; nicotine, n = 27) and noncartilaginous (control, n = 32; nicotine, n = 32) airway wall per unit epithelial basement membrane. (*B*) mRNA expression in cartilaginous (control, n = 22; nicotine, n = 27) and noncartilaginous (control, n = 32; nicotine, n = 32) airway wall per unit wall area. (*C*) Protein accumulation in cartilaginous (control, n = 19; nicotine, n = 29) and membranous (control, n = 24; nicotine, n = 27) and terminal (control, n = 19; nicotine, n = 20) airway wall per unit epithelial basement membrane. (*D*) Protein expression in cartilaginous (control, n = 19; nicotine, n = 29) and membranous (control, n = 24; nicotine, n = 27) and terminal (control, n = 19; nicotine, n = 20) airway wall per unit wall area. *$P < 0.05$. *Open bars*, control; *solid bars*, nicotine.

around the tips of the secondary crests or at the mouths of primitive alveoli (Figure 5). *In situ* hybridization and immunohistochemical analysis of collagen α1(III) mRNA are shown in Figures 4A and 4B; elastin is shown in Figures 5A and 5B. As can be seen in Figure 4, prenatal nicotine exposure increases collagen mRNA expression in the parenchyma. This was quantified as the number of grains per unit of alveolar area, and that measure was corrected for volume density of alveolar wall to normalize for changes in respiratory unit structures following nicotine treatment and for variations with in the groups. Cells at the tips of the secondary crests expressed both collagen and elastin, whereas alveolar wall interstitial cells and mesothelial cells expressed both collagen types but little elastin (Figures 4 and 5).

Collagen type I, collagen type III, and elastin density of silver grains per unit area corrected for volume density of alveolar wall increased (46, 117, and 62%, respectively) significantly ($P < 0.5$) following nicotine exposure (Table 2). The number of grains per unit alveolar area for collagen III and elastin was also higher in the nicotine treatment group (103 and 52%, respectively; $P < 0.03$) (Table 2). Values of collagen type I and type III immunostaining intensity per unit alveolar area were significantly higher (134 and 75%, respectively) in the nicotine-treated group than in the control group (Table 3 and Figures 4C–4F). Values of intensity per unit area corrected for volume density of alveolar wall were also higher for both collagen I and III (166 and 94%, respectively) in the nicotine-treated group (Table 3). In contrast to collagen, and in contrast to the increased levels of elastin mRNA, elastin immunostaining intensity per unit area or per unit area corrected for volume density of alveolar wall was not increased (Figure 5). Levels of elastin protein were actually slightly decreased (45 and 29%, respectively) in the nicotine-treated group, but these changes did not reach a level of significance (Figure 5 and Table 3).

Whole-Lung Collagen mRNA Levels

To further confirm the effects of prenatal nicotine exposure on collagen mRNA levels and to correlate the changes in collagen expression with changes in pulmonary function, a second set of timed-pregnant monkeys was treated with nicotine (1.5 mg/kg/d) from Days 28–160 of gestation (term = 165 d), delivered by cesarean section on Day 160, and then subjected to pulmonary function tests the following day and killed. Lung RNA was prepared from the right upper lobe, and collagen α1(I), α1(III), and α2(V) were measured by real-time PCR. As shown in Figure 6, collagen RNA levels were significantly increased by nicotine treatment. Associated with these increases in collagen mRNA in newborn monkey lung were alterations in pulmonary function as measured by increased pulmonary resistance and decreased expiratory flows. These effects of prenatal nicotine exposure on pulmonary function are described in detail elsewhere (14).

Colocalization of collagen and α7 nAChR. The similar expression patterns of α7 nAChR and collagen shown in Figure 1 strongly suggest their coexpression by fibroblasts. This was confirmed by dual labeling studies and by isolation of pulmonary fibroblasts. Dual immunohistochemical staining for α7 nAChR and *in situ* hybridization for collagen mRNA showed coexpression in cells in the paracartilaginous region of airways (Figure 7A). Combined fluorescent ligand binding and immunohistochemical staining showed that the α7 nAChRs present on airway wall cells were able to bind their specific ligand α-Bungarotoxin and

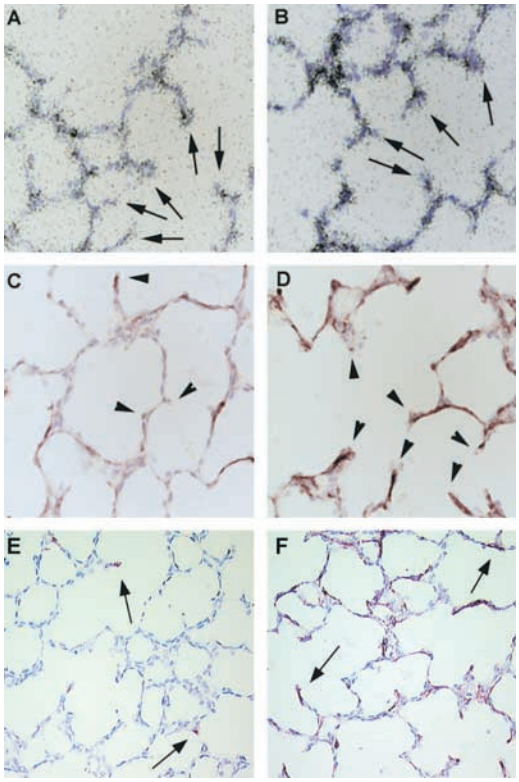

Figure 4. In situ hybridization and immunohistochemical analyses of collagen type α1(I) and α1(III) expression in lung parenchyma following fetal nicotine exposure during pregnancy. (*A*) Bright-field image of antisense ^{35}S-labeled cRNA probe showing collagen α1(I) mRNA expression in control 134-d fetal lung parenchyma. (*B*) Bright-field image of α1(III) mRNA expression in nicotine-exposed fetal lung. (*C*) Immunostaining of control 134-d fetal lung using collagen type I monoclonal antibody and stained with AEC (*see* MATERIALS AND METHODS). (*D*) Collagen I immunostaining of nicotine-treated fetal lung. (*E*) Immunostaining of control 134-d fetal lung using collagen type III monoclonal antibody and stained with AEC. (*F*) Collagen III immunostaining of nicotine-treated fetal lung. *Arrows* point to collagen mRNA expression in cells located on the tips of septal crests and to collagen fibers identified with immunohistochemistry in septal crests and alveolar walls. *A*—*D*, 630×; *E* and *F*, 500×.

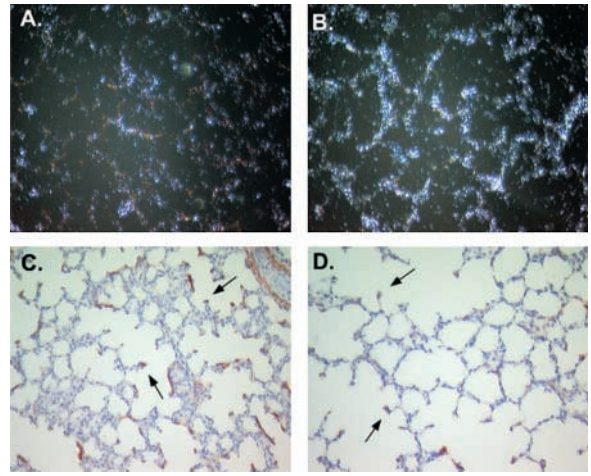

Figure 5. In situ hybridization and immunohistochemical analyses of the effect of prenatal nicotine on elastin expression in lung parenchyma. (*A*) Dark-field image of antisense ^{35}S-labeled cRNA probe showing elastin mRNA expression in control 134-d fetal lung parenchyma. (*B*) Dark-field image of elastin mRNA expression in nicotine-treated fetal lung. (*C*) Immunostaining of control fetal lung using antihuman elastin polyclonal antisera and stained with AEC (*see* MATERIALS AND METHODS). (*D*) Elastin immunostaining of nicotine-treated fetal lung. *Arrows* show elastin staining was predominantly located at the tips of secondary septi or at the mouths of primitive alveoli opening into alveolar ducts. All sections, 400×.

that abundant collagen deposition was found around these cells (Figures 7B and 7C). In addition to airway wall cells, α-Bungarotoxin binding was also evident in airway epithelial cells, smooth muscle cells, and submucous gland cells (Figure 7A). To further confirm the coexpression of α7 nAChR and collagen, primary cell cultures of fibroblasts were established. As shown in Figure 8, isolated fibroblasts from fetal monkey lung express α7 mRNA and collagen α1(III) mRNA and immunostain for α7 nAChR and procollagen III. These findings suggest that the direct interaction of nicotine with α7 nAChR expressed on fibroblasts leads to altered collagen gene expression.

Discussion

Adverse effects of maternal smoking during pregnancy, including premature birth, diminished somatic growth, neonatal morbidity and mortality, and increased incidence of respiratory ailments and hospitalization, have been well documented (1, 2, 4). Multiple studies have linked gestational cigarette exposure as opposed to postnatal exposure to abnormal infant lung function (5–7, 9). However, the underlying mechanisms by which gestational smoke exposure causes structural and functional changes in infant lungs remain poorly understood. Recently, we reported the presence of abundant expression of nAChR subunits in the developing lung suggesting a logical mechanism by which smoking during pregnancy may effect lung development.

Nicotine readily crosses the feto–placental barrier and attains amniotic fluid levels equivalent or higher than maternal serum nicotine levels (19, 20). The typical dose of heavy human smokers is ~ 1 mg/kg/d; typically, nicotine patches and gum deliver half and one quarter the nicotine dose of smoking, respectively (21). To model this, nicotine was delivered to pregnant monkeys via osmotic minipumps from Day 26–134 of gestation at a dose of 1 mg/kg/d. Amniotic fluid nicotine levels (15.4 ± 3.9 ng/ml; 95 nM) were in the mid-range observed in amniotic fluid of human smokers (16, 19). Monkeys were delivered by cesarean section at 134 d of gestation (term = 165 d), which is approximately equivalent to 32 wk of human gestation. This period was chosen to investigate the effect of maternal nicotine on fetal lung cellular differentiation and structural remodeling during the late saccular phase of lung development. A second set of monkeys was delivered at 160 d (just before full-term pregnancy) to allow pulmonary function testing. These animals received 1.5 mg/kg/d nicotine

TABLE 2

Effect of prenatal nicotine exposure on collagen type I, collagen type III and elastin mRNA expression in fetal alveolar wall

Parameter	Control	Nicotine	*P* Value
Collagen type I			
Grains/mm^2 area	1,450.4 ± 182.6	2,015.4 ± 223.2	0.06
Grains/mm^2 alveolar wall area	5,023.1 ± 687.1	7,369.1 ± 502.7	0.025
Collagen type III			
Grains/mm^2 area	544.3 ± 22.9	1,106.1 ± 138.5	0.008
Grains/mm^2 alveolar wall area	1,882.1 ± 124.7	4,088.0 ± 584.27	0.01
Elastin			
Grains/mm^2 area	1,393.8 ± 89.3	2,128.1 ± 206.4	0.015
Grains/mm^2 alveolar wall area	4,854.5 ± 590.1	7,864.8 ± 914.4	0.025

* Values are means ± SE.

because amniotic fluid nicotine levels obtained in the first set of animals was not as high as is observed in heavy smokers (16, 19). At 140 d gestation, these animals had amniotic nicotine levels of 17.7 ± 8.7 ng/ml (110 nM).

In the present study, prenatal nicotine exposure increased airway wall area in cartilaginous membranes and terminal airways. This nicotine-induced increase in airway wall area was significant both as normalized to per unit basement membrane and by linear regression analysis comparing airway wall area to airway diameter. The proportion of cartilage area remained unchanged (data not shown) following nicotine exposure. Elliot and colleagues (22) observed a similar increase in inner airway wall thickness defined as area inclusive of epithelium and outer limits of smooth muscular layer in cartilaginous airways in sudden infant death syndrome subjects whose mothers smoked during and after pregnancy. The mean age of these smoke-exposed sudden infant death syndrome cases was 5 mo, ranging from 1–18 mo. These investigators were unable to isolate the effect of prenatal smoke exposure from that of postnatal exposure. Although we did not measure airway wall thickness exactly as did Elliot, our findings are in concert with their observation that smoking during pregnancy produces changes in airway wall dimensions. However, our findings suggest that nicotine must be the factor responsible for increasing airway wall dimensions in infants of mothers who smoke during pregnancy.

Airway walls, particularly para- and extracartilaginous areas, are host predominantly to fibroblasts that are primarily involved in connective tissue protein synthesis (23). In the lung, collagen comprises 15–20% of dry lung weight. Although there are eleven different types of collagen found in the lung, collagen type I and type III are the most abundant and account for more than 90% of lung collagen content (17). After nicotine exposure from Day 26–134, collagen type I and III mRNA expression and immunostaining intensity were increased significantly in both cartilaginous and noncartilaginous airways. The percentage increase of collagen type I and III mRNA expression and immunostaining was relatively greater in distal airways than in central airways. Not only did collagen mRNA and protein expression increase per unit epithelial membrane, but it also increased per unit area. Per unit basement membrane increase is expected if the thickness of the airway wall is increased and collagen equilibrium is maintained. However, an increase in per unit area indicates that nicotine upregulated both collagen gene expression and protein deposition in airway walls. Similar increases in collagen type I, III, and V mRNA expression measured by real-time RT-PCR were also observed in 1-d-old infants that were exposed *in utero* to nicotine from Day 26–160 (Figure 6).

Our data suggest that nicotine may increase collagen via the α7 nAChR. We have previously reported that maternal nicotine exposure in monkeys upregulated α7 nAChRs expression in cartilaginous airway walls and that α7 nAChR are in abundance in the perichondral areas where the density of fibroblasts is highest (16). No other nicotinic receptor subtypes were detected in this region (16). In this pa-

TABLE 3

Effect of prenatal nicotine exposure on collagen type I, collagen type III, and elastin deposition in fetal alveolar walls

Parameter	Control	Nicotine	*P* Value
Collagen type I			
Integrated intensity/μm^2 area	0.55 ± 0.04*	1.29 ± 0.28	0.029
Integrated intensity/μm^2 alveolar wall area	1.99 ± 0.26	5.30 ± 1.29	0.033
Collagen type III			
Integrated intensity/μm^2 area	1.91 ± 0.24	3.36 ± 0.46	0.024
Integrated intensity/μm^2 alveolar wall area	6.96 ± 1.19	13.55 ± 1.20	0.008
Elastin			
Integrated intensity/μm^2 area	1.09 ± 0.19	0.78 ± 0.10	0.11
Integrated intensity/μm^2 alveolar wall area	3.89 ± 0.69	3.14 ± 0.26	0.19

* Values are means ± SE.

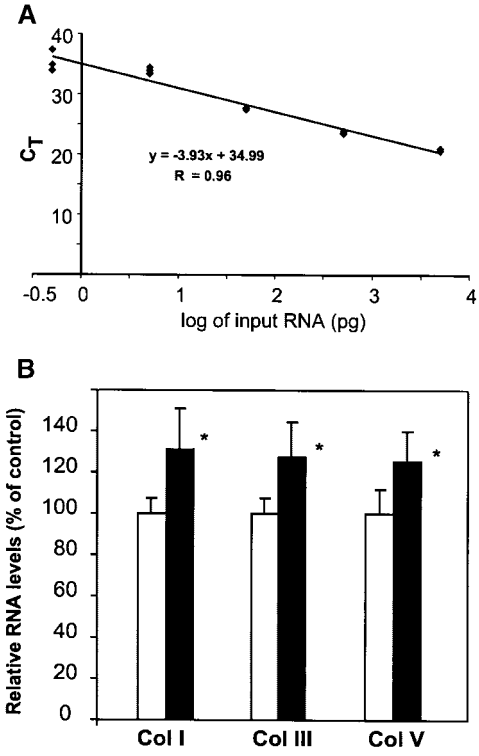

Figure 6. (*A*) Standard curve used for analysis of collagen I plotting obtained CT values for 0.5–5,000 pg input RNA. (*B*) Real-time PCR analysis of collagen type α1(I), α1(III), and α2(V) mRNA levels in lungs from 1-d-old monkeys. *Open bars*, controls; *solid bars*, prenatal nicotine exposure from Days 28–160 gestation (1.5 mg/kg/d). Relative RNA levels are normalized for each collagen subtype. $*P < 0.01$ for nicotine exposure compared with control animals by one-way ANOVA.

per, by dual α7 receptor immunohistochemistry combined with *in situ* hybridization for collagen III, and by dual collagen III immunohistochemistry combined with αBGT binding, we show that the same cells in the airway wall appear to express both collagen and α7 nAChR. In addition, isolated pulmonary fibroblasts clearly express both α7 nAChR and collagen III. Thus, expression of α7 nAChR in pulmonary fibroblasts has been unambiguously demonstrated. Although clear causality between nicotine's interaction with α7 receptors and collagen expression remains to be proven in cell culture systems, these observations suggest that the interaction of nicotine with α7 receptors underlies the effects of nicotine (and smoking) on collagen expression. For this to be true, the concentration of nicotine that the fetus is exposed to must be sufficient to interact with the α7 receptor. Typically, the concentration of chronic nicotine exposure to inactivate/desensitize nicotinic receptors is less than the concentration needed for activation. Olale and colleagues (24) have demonstrated that the IC50 for inactivation of human α7 receptors expressed in *Xenopus* oocytes is 2.8 nM, whereas the EC50 for activation is greater than 40 μM. Given that the human fetus whose mother smokes is exposed to concentrations of nicotine ranging from 5–200 nM, it is clear that concentrations of nicotine in the fetus are not nearly high enough to activate the α7 receptor but that levels are high enough, even during the night, to inactivate the α7 receptor. Inactivation of α7 receptors is also consistent with our observations of nicotine-induced increases in α7 nAChR levels (Figures 6A and 6B) as *in vitro* studies have demonstrated that chronic exposure of both cell lines (25) and *Xenopus* oocytes (24) expressing the α7 receptor leads to increased levels of inactivated receptor.

Because the α7 receptor is primarily a ligand-gated calcium channel (15), activation of the α7 receptor leads to increased intracellular calcium and inhibition of the α7 receptor leads to decreased intracellular calcium. Linking intracellular calcium to collagen gene expression, Flaherty and Chojkier (26) have shown that increased intracellular calcium decreases collagen gene biosynthesis in human fibroblasts (26). This is consistent with our data and supports the hypothesis that prenatal nicotine exposure leads to inactivated α7 receptors, decreased fibroblast intracellular calcium, and therefore increased collagen. It is important to point out that there are also likely to be effects on collagen degradation. For example, Genbacev and colleagues (27) have reported that *in vitro* nicotine lowers activity of 92-kDa type IV collagenase in cytotrophoblasts. Therefore, it is likely that the increased collagen levels in the nicotine-exposed fetal lungs results from both increased collagen synthesis and from decreased degradation. Nicotine may also modulate collagen synthesis through intermediates such as tumor growth factor-β or fibroblast growth factor. Clearly, *in vitro* studies are needed to explore these mechanisms.

Not only were collagen type I and III mRNA expression and immunostaining increased in airway walls, but a similar increase was also observed in alveolar walls. During development, connective tissue proteins form a three–dimensional, semi-rigid scaffold that serves as the basic framework for the acinar development (23). Synthesis, maturation, and deposition of collagen and elastin fibers at or around the secondary crest tips are essential for the subdivision of gas exchanging units to alter the surface complexity of lung (17). Thus, alterations in this connective tissue scaffold might alter the surface complexity of lung. Consistent with this, we found a decrease in alveolar surface area and an increase in alveolar size following nicotine exposure (16). Similarly, in rodents, prenatal cigarette smoke (28) or a combination of prenatal and postnatal nicotine exposure (29) decreases alveolar septation and the number of respiratory units.

Elastin mRNA expression was localized in the subepithelial compartment and around the smooth muscle layer where α7 nAChRs expression is rather low compared with that of perichondrial regions. This raises the possibility that elastin may be regulated by other nAChR subtypes present in those regions. It is surprising that, whereas elastin mRNA expression in alveolar walls was increased after *in utero* nicotine exposure, organized elastin (α-elastin fraction of insoluble elastin) was slightly decreased (19%; not significant) (Figures 5C and 5D). A reduction in elastic tissue content has also been reported in rat pups exposed to nicotine from Day 7 of gestation to Week 3 of postnatal life (30). These findings suggest that after elastin gene induction, elastin protein deposition does not increase to the

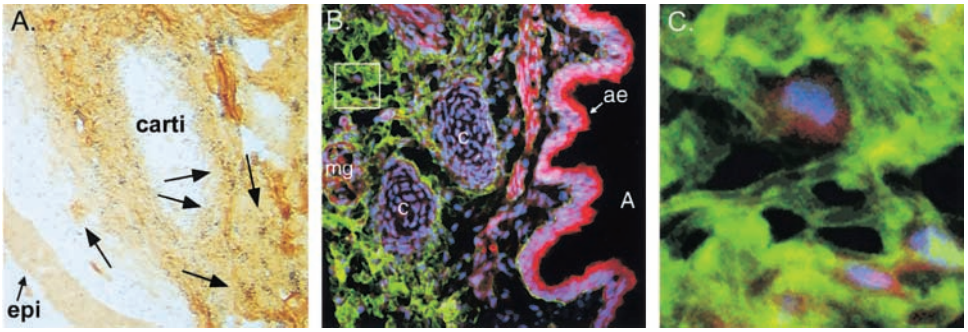

Figure 7. Coexpression of α7 nAChR and collagen in 134-d fetal monkey lung. (*A*) Dual α7 nAChR immunostaining (chromogen = DAB) and collagen α1(III) *in situ* hybridization. Lung sections were stained with antihuman α7 nAChR (mAb 319) and then hybridized with collagen type III probe (*see* MATERIALS AND METHODS). α7 nAChR staining and collagen mRNA expression colocalize in airway wall cells. (*B* and *C*). Confocal colocalization of collagen III and αBGT binding sites. Sections were treated with collagen type III antibody and then incubated in a cocktail of Texas-red–conjugated α-BGT and fluorescein-conjugated secondary antibody at 37°C for 3 h. Nuclei were counterstained with DAPI (*blue*). (*B*) α-BGT binding (*red*) in airway wall cells, smooth muscle cells, submucous gland cells, and airway epithelial cells; collagen staining (*green*); overlap of red and green channels (*yellow*). (*C*) High-power view showing that cells with abundant αBGT binding are surrounded by collagen in the airway wall.

same extent. It may occur due to mRNA degradation, alternate splicing, translation problems, inhibition of crosslinking, or increased elastin degradation and remains to be investigated. Interestingly, in adult smokers, whereas collagen is increased, elastin is decreased in emphysematous lung parenchyma tissue compared with nonsmokers (31), suggesting that nicotine may alter connective tissue equilibrium via the same pathways both during pre- or postnatal age. Laurent and colleagues (32) showed that filtered smoke inhibited elastin cross-linking in the lung *in vitro*. In adults, cigarette smoke is known to increase elastase production and its activity. It is likely that elastin remodeling may be regulated by a different pathway than that of collagen in developing lungs.

The fixed lung volume in nicotine-exposed fetuses was significantly decreased (16), and a similar decrease in lung volume has also been reported in rats following gestational cigarette smoke exposure (28). Fixed lung volume is independent of surface tension forces and is determined mainly by cellular and connective tissue components. In humans, collagen type III, which is considered responsible for compliance, is 30% of the total collagen, whereas collagen type I, which renders rigidity and tensile strength, is 60% of total lung collagen at birth (17). We found a significant increase in collagen mRNA and protein expression following nicotine exposure in all compartments of lung. It is likely that in addition to structural hypoplasia(16, 28), excessive collagen accumulation may also be responsible for the decrease in fixed lung volume. In addition, higher collagen content may also explain the small decrease in functional residual capacity observed in *in utero* smoke-exposed babies (8). A number of studies have documented that infants whose mothers smoke during pregnancy have decreased lung compliance (6, 7). Although lung compliance is determined by a complex interaction of multiple components in the lung, we infer that an increase in collagen deposition in the lung parenchyma may also contribute to a decrease in lung compliance in infants whose mothers smoke during gestation.

Epidemiologic studies have reported that children of mothers who are habitual smokers during pregnancy and/or afterward also have reduced expiratory flow rates (8–10), reduced T_{PTEF}:T_E (8), and increased respiratory resistance (6). In the present study, nicotine augmented collagen type I and III accumulation in the airway walls, an increase that interestingly increased proportionately more in peripheral than in central airway generations. Given that changes in the peripheral airway dimensions produce greater alterations in airway resistance and maximum ex-

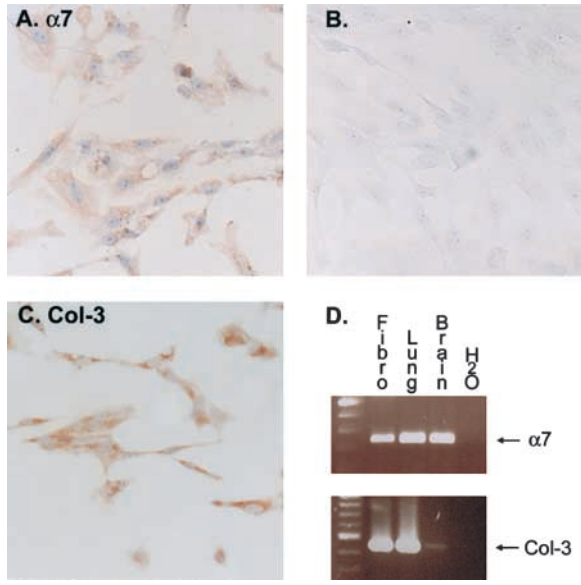

Figure 8. Coexpression of α7 nAChR and collagen in isolated pulmonary fibroblasts. Fibroblasts were isolated from 100-d fetal monkey lung as described in MATERIALS AND METHODS. (*A*) Immunohistochemistry for α7 nAChR using monoclonal antibody 319. (*B*) Nonimmune serum control for (*A*). (*C*) Immunohistochemistry for procollagen III. Panels *A*—*C*, 200×; chromogen = AEC. (*D*) RT-PCR analysis of RNA prepared from cultured fibroblasts. *Upper panel* shows amplified bands using monkey α7 nAChR primers; *lower panel* shows amplified bands using monkey collagen α1(III) primers. *Arrows* point to bands of predicted size. Fibro, RNA from cultured fibroblasts; Lung, RNA from newborn monkey lung; Brain, RNA from monkey forebrain; H2O, no input DNA.

piratory flow rates than changes in central airways, the morphometric alterations in airway wall dimensions and increased collagen accumulation reported here may provide explanations for the altered pulmonary functions observed in infants of mothers who smoked during pregnancy (6, 8–10).

There are several additional comments that are important. First, it is important to keep in mind that the effects and mechanisms of maternal smoking on lung development are likely to be very different from the effects of adult smoking on adult lung. One is an indirect effect of only those compounds that diffuse into blood and cross the placenta, whereas the other is a direct effect of everything in cigarette smoke. Second, the duration of the effect of prenatal nicotine is unknown but likely lasts into adolescence (9, 33) or beyond (13). Finally, the marked sensitivity of the $\alpha 7$ receptor for inhibition by nicotine (ED50 = 2.8 nM) makes it possible that even the lower doses of nicotine obtained from a nicotine patch or gum, which still raise nicotine blood levels to greater than 80 and 40 nM, respectively (34, 35), will effect lung development during pregnancy.

In summary, nicotine exposure during pregnancy not only increased airway wall thickness, but it also stimulated the synthesis and accumulation of collagen type I and III in airway walls and alveolar compartments. These alterations may in part contribute to the observed lung function abnormalities in *in utero* smoke-exposed infants. This direct evidence of adverse effects of nicotine on the developing fetus further supports the need for active counseling and aggressive campaigns against smoking during pregnancy.

Acknowledgments: The authors thank Dr. Anda Cornea for guidance with image analysis and confocal microscopy; Dr. John Fanton, Darla Jacob, and Roger Simons of the Oregon Regional Primate Research Center (ORPRC) of Division of Animal Resources for assistance with timed-pregnant monkeys; and Yibing Jia of the ORPRC Molecular Biology Core for assistance in preparation of the collagen and elastin cDNA probes. This research was supported by National Institute of Health grants RR-00163 and HD/HL-37131.

References

1. Cliver, S. P., R. L. Goldenberg, G. R. Cutter, H. J. Hoffman, R. O. Davis, and K. G. Nelson. 1995. The effect of cigarette smoking on neonatal anthropometric measurements. *Obstet. Gynecol.* 85:625–630.
2. Wen, S. W., R. L. Goldenberg, G. R. Cutter, H. J. Hoffman, S. P. Cliver, R. O. Davis, and M. B. DuBard. 1990. Smoking, maternal age, fetal growth, and gestational age at delivery. *Am. J. Obstet. Gynecol.* 162:53–58.
3. Mathews, T. J. 1998. Smoking during pregnancy, 1990–96. *Natl. Vital. Stat. Rep.* 47:1–12.
4. Taylor, B., and J. Wadsworth. 1987. Maternal smoking during pregnancy and lower respiratory tract illness in early life. *Arch. Dis. Childhood* 62:786–791.
5. Tager, I. B., J. P. Hanrahan, T. D. Tosteson, R. G. Castile, R. W. Brown, S. T. Weiss, and F. E. Speizer. 1993. Lung function, pre- and post-natal smoke exposure, and wheezing in the first year of life. *Am. Rev. Respir. Dis.* 147:811–817.
6. Milner, A. D., M. J. Marsh, D. M. Ingram, G. F. Fox, and C. Susiva. 1999. Effects of smoking in pregnancy on neonatal lung function. *Arch. Dis. Child Fetal Neonatal. Ed.* 80:F8–F14.
7. Lodrup Carlsen K. C., J. J. Jaakkola, P. Nafstad, and K. H. Carlsen. 1997. In utero exposure to cigarette smoking influences lung function at birth. *Eur. Respir. J.* 10:1774–1779.
8. Tager, I. B., L. Ngo, and J. P. Hanrahan. 1995. Maternal smoking during pregnancy: effects on lung function during the first 18 months of life. *Am. J. Respir. Crit. Care Med.* 152:977–983.
9. Cunningham, J., D. W. Dockery, and F. E. Speizer. 1994. Maternal smoking during pregnancy as a predictor of lung function in children. *Am. J. Epidemiol.* 139:1139–1152.
10. Hanrahan, J. P., I. B. Tager, M. R. Segal, T. D. Tosteson, R. G. Castile, H. Van Vunakis, S. T. Weiss, and F. E. Speizer. 1992. The effect of maternal smoking during pregnancy on early infant lung function. *Am. Rev. Respir. Dis.* 145:1129–1135.
11. Dezateux, C., J. Stocks, I. Dundas, and M. E. Fletcher. 1999. Impaired airway function and wheezing in infancy: the influence of maternal smoking and a genetic predisposition to asthma. *Am. J. Respir. Crit. Care Med.* 159:403–410.
12. Hoo, A. F., M. Henschen, C. Dezateux, K. Costeloe, and J. Stocks. 1998. Respiratory function among preterm infants whose mothers smoked during pregnancy. *Am. J. Respir. Crit. Care Med.* 158:700–705.
13. Upton, M. N., G. C. Watt, G. D. Smith, A. McConnachie, and C. L. Hart. 1998. Permanent effects of maternal smoking on offspring's lung function. *Lancet* 352:453–453.
14. Sekhon, H. S., J. A. Keller, N. L. Benowitz, and E. R. Spindel. 2001. Prenatal nicotine exposure alters pulmonary function in newborn rhesus monkeys. *Am. J. Respir. Crit. Care Med.* 164:989–994.
15. Lindstrom, J. 1997. Nicotinic acetylcholine receptors in health and disease. *Mol. Neurobiol.* 15:193–222.
16. Sekhon, H. S., Y. Jia, R. Raab, A. Kuryatov, J. F. Pankow, J. A. Whitsett, J. Lindstrom, and E. R. Spindel. 1999. Prenatal nicotine increases pulmonary alpha7 nicotinic receptor expression and alters fetal lung development in monkeys. *J. Clin. Invest.* 103:637–647.
17. Chambers, R. C., and G. J. Laurent. 1997. Collagens. *In* The Lung: Scientific Foundations. 2nd ed. R. G. Crystal and J. B. West, editors. Raven, Philadelphia. 709–727.
18. Schoepfer, R., W. G. Conroy, P. Whiting, M. Gore, and J. Lindstrom. 1990. Brain alpha-bungarotoxin binding protein cDNAs and MAbs reveal subtypes of this branch of the ligand-gated ion channel gene superfamily. *Neuron* 5:35–48.
19. Luck, W., H. Nau, R. Hansen, and R. Steldinger. 1985. Extent of nicotine and cotinine transfer to the human fetus, placenta and amniotic fluid of smoking mothers. *Dev. Pharmacol. Ther.* 8:384–395.
20. Luck, W., and H. Nau. 1984. Exposure of the fetus, neonate, and nursed infant to nicotine and cotinine from maternal smoking. *N. Engl. J. Med.* 311:672–672.
21. Benowitz, N. L. 1988. Pharmacologic aspects of cigarette smoking and nicotine addiction. *N. Engl. J. Med.* 319:1318–1330.
22. Elliot, J., P. Vullermin, and P. Robinson. 1998. Maternal cigarette smoking is associated with increased inner airway wall thickness in children who die from sudden infant death syndrome. *Am. J. Respir. Crit. Care Med.* 158: 802–806.
23. Thurlbeck, W. M. 1995. Lung growth and development. *In* Pathology of the Lung. 2nd ed. W. M. Thurlbeck and A. M. Churg, editors. Thieme Medical Publishers, New York. 37–88.
24. Olale, F., V. Gerzanich, A. Kuryatov, F. Wang, and J. Lindstrom. 1997. Chronic nicotine exposure differentially affects the function of human $\alpha 3$, $\alpha 4$, and $\alpha 7$ neuronal nicotinic receptor subtypes. *J. Pharmacol. Exp. Ther.* 283:675–683.
25. Ke, L., C. M. Eisenhour, M. Bencherif, and R. J. Lukas. 1998. Effects of chronic nicotine treatment on expression of diverse nicotinic acetylcholine receptor subtypes: I. Dose- and time-dependent effects of nicotine treatment. *J. Pharmacol. Exp. Ther.* 286:825–840.
26. Flaherty, M., and M. Chojkier. 1986. Selective inhibition of collagen synthesis by the Ca2+ ionophore A23187 in cultured human fibroblasts. *J. Biol. Chem.* 261:12060–12065.
27. Genbacev, O., K. E. Bass, R. J. Joslin, and S. J. Fisher. 1995. Maternal smoking inhibits early human cytotrophoblast differentiation. *Reprod. Toxicol.* 9:245–255.
28. Collins, M. H., A. C. Moessinger, J. Kleinerman, J. Bassi, P. Rosso, A. M. Collins, L. S. James, and W. A. Blanc. 1985. Fetal lung hypoplasia associated with maternal smoking: a morphometric analysis. *Pediatr. Res.* 19:408–412.
29. Maritz, G. S., and R. A. Thomas. 1994. The influence of maternal nicotine exposure on the interalveolar septal status of neonatal rat lung. *Cell Biol. Int.* 18:747–757.
30. Maritz, G. S., and K. Woolward. 1992. Effect of maternal nicotine exposure on neonatal lung elastic tissue and possible consequences. *S. Afr. Med. J.* 81:517–519.
31. Cardoso, W. V., H. S. Sekhon, D. M. Hyde, and W. M. Thurlbeck. 1993. Collagen and elastin in human pulmonary emphysema. *Am. Rev. Respir. Dis.* 147:975–981.
32. Laurent, G. J., and R. J. McAnulty. 1983. Protein metabolism during bleomycin-induced pulmonary fibrosis in rabbits: *in vivo* evidence for collagen accumulation because of increased synthesis and decreased degradation of the newly synthesized collagen. *Am. Rev. Respir. Dis.* 128:82–88.
33. Rantakallio, P. 1983. A follow-up study up to the age of 14 of children whose mothers smoked during pregnancy. *Acta Paediatr. Scand.* 72:747–753.
34. Benowitz, N. L., and S. G. Gourlay. 1997. Cardiovascular toxicity of nicotine: implications for nicotine replacement therapy. *J. Am. Coll. Cardiol.* 29:1422–1431.
35. Nilsson, P., H. Lundgren, M. Soderstrom, K. O. Fagerstrom, and P. Nilsson-Ehle. 1996. Effects of smoking cessation on insulin and cardiovascular risk factors: a controlled study of 4 months' duration. *J. Intern. Med.* 240:189–194.